Sphere to Rod Transition of Micelles Formed by Amphiphilic Diblock Copolymers of Vinyl Ethers in Aqueous Solution

Minoru Nakano, Hideki Matsuoka, and Hitoshi Yamaoka*

Department of Polymer Chemistry, Kyoto University, Kyoto 606-8501, Japan

Andreas Poppe and Dieter Richter

Institut für Festkörperforschung, Forschungszentrum Jülich GmbH, D-52425 Jülich, Germany

Received August 27, 1998; Revised Manuscript Received December 4, 1998

ABSTRACT: Amphiphilic block copolymers of vinyl ethers containing 2-hydroxyethyl vinyl ether (HOVE) and partially deuterated *n*-butyl vinyl ether (NBVE) were synthesized by living cationic polymerization. Four block copolymers with the same hydrophilic length but different hydrophobic lengths were prepared. The internal structures of the micelles formed by these copolymers in aqueous solution were investigated by the contrast variation method of small-angle neutron scattering (SANS) measurement. The molar volume of HOVE was estimated to be quite small from the dependence of the forward scattering intensity on the contrast, which comes from the hydration effect in the micellar shell. The SANS data were well described by the theoretical form factor of a core−shell model. The micellar shape was strongly dependent on the hydrophobic chain length of the block copolymer. The polymer with the shortest hydrophobic chain was suggested to form spherical micelles, whereas the scattering curves of the longer hydrophobic chain polymers showed the q^{-1} dependence, reflecting the formation of rodlike micelles. These scattering curves could be described well by a sphere−rod coexistence model. The volume fraction of the rodlike micelle was found to increase with increasing hydrophobic chain length.

1. Introduction

Amphiphilic copolymers which are widely used in industrial fields are also important materials in many fields of natural science such as colloid science and biology. Many groups have studied the specific behavior of amphiphilic polymers such as micellar formation and adsorption in selective solvents during the past few decades.[1−4]

Quantitative theoretical approaches demand the synthesis of amphiphilic polymers with a well-defined structure. Living polymerization is the most important and powerful technique for this purpose. Indeed, most nonionic amphiphilic block copolymers, which have an oxyethylene chain as a hydrophilic segment, are synthesized by living anionic polymerization[5] in order to obtain a narrow molecular weight distribution and a controlled molecular weight.

Sawamoto et al. have reported the living cationic polymerization of alkyl vinyl ethers,[6,7] and they synthesized an amphiphilic block copolymer with 2-hydroxyethyl vinyl ether as a hydrophilic part. This new polyalcohol-type amphiphile can be a valuable sample along with the oxyethylene-type nonionic block copolymer for investigation of its specific phenomena, since it can be prepared with a precise control of molecular weight using relatively simple equipment.

Small-angle neutron scattering (SANS), which has been reported by many groups,[2,8−13] is a valuable method for evaluation of the internal structure of micelles. Since the neutron is scattered by the density fluctuation of scattering length inherent for each atom, and an atom (proton, for example) has a different scattering length from its isotope (deuterium), SANS measurement makes it possible to investigate the heterogeneity of the internal structure of the micelle by use of a hydrogenated/deuterated mixture. This so-called contrast variation method[14,15] is applicable to the system with enough contrast inside the particle, which means that, in the case of a micellar system, partial deuteration is needed to obtain a large contrast of the scattering length density (SLD) between the core and the shell of the micelle. An alkyl vinyl ether monomer with a deuterated alkyl group can be prepared by the palladium-catalyzed ether exchange reaction with deuterated alcohol.[16] Thus, amphiphilic block copolymers of vinyl ethers are quite useful materials for the investigation of their micellar structure by means of SANS.[11]

Here, we have investigated the behavior of amphiphilic block copolymers synthesized by living cationic polymerization in aqueous solution and have determined the size and shape of the micelles by the SANS technique. We report the transition of the micellar shape from sphere to rod with increasing molar fraction of hydrophobic part in a polymer.

2. Experimental Section

Synthesis of Amphiphilic Diblock Copolymers. Block copolymers were synthesized by living cationic polymerization with two kinds of monomers, 2-acetoxyethyl vinyl ether (AcOVE) and *n*-butyl vinyl ether (NBVE), as shown in Scheme 1. AcOVE can be led to water-soluble 2-hydroxyethyl vinyl ether (HOVE) by hydrolysis of the protective group after polymerization. The AcOVE monomer was synthesized from sodium acetate (98.5%, Nacalai tesque, Kyoto) and 2-chloroethyl vinyl ether (99%, Aldrich, Milwaukee) at 90 °C. As a hydrophobic segment, a mixture of *n*-butyl-d_9 vinyl ether and *n*-butyl-h_9 vinyl ether was used for two purposes. One was to obtain enough contrast between hydrophilic and hydrophobic segments for neutron scattering, and the other was to achieve high accuracy for determination of the polymer composition by ^{1}H NMR spectroscopy. *n*-Butyl-d_9 vinyl ether was synthesized from octadecyl vinyl ether (Tokyo Kasei, Tokyo) and *n*-butanol-d_{10} (99.5 at. % D, C/D/N Isotopes, Quebec) by the ether exchange reaction with 1,10-phenanthroline palladium

* To whom correspondence should be addressed.

10.1021/ma981351p CCC: $18.00 © 1999 American Chemical Society
Published on Web 01/15/1999

Scheme 1. Synthesis of Poly(HOVE-*b*-NBVE)

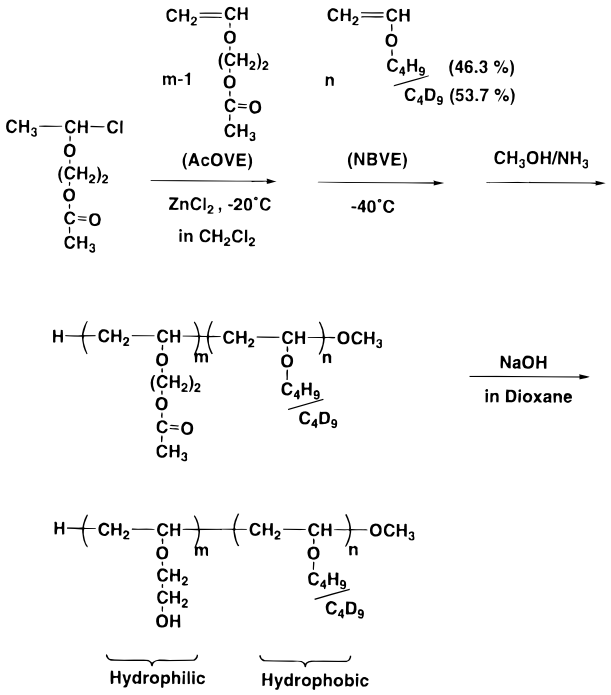

diacetate as a catalyst. This monomer and commercial NBVE (Nacalai tesque) were mixed and then distilled before polymerization. The molar fraction of the deuterated monomer in the NBVE mixture was determined to be 0.537 by ^{1}H NMR. The hydrogen chloride adduct of AcOVE was obtained by bubbling the hydrogen chloride gas into a hexane solution of AcOVE. Commercial zinc chloride as diethyl ether solution (Aldrich) was used without further purification.

Polymerization was performed in a dried flask with a three-stopcock under nitrogen. We started five batches simultaneously, to prepare four block copolymers with the same hydrophilic length and a different hydrophobic length. The hydrogen chloride adduct of AcOVE and zinc chloride was injected as an initiator system into the dichloromethane solution of AcOVE at −20 °C. When the AcOVE monomer conversion determined by gas chromatography reached 95%, one batch was quenched by ammoniacal methanol; simultaneously, a different amount of NBVE monomer was added to the other four reaction solutions at −40 °C. The copolymerization was terminated by injection of ammoniacal methanol.

Table 1. Molecular Characteristics of Poly(HOVE-*b*-NBVE)

	m^a	n^b	$M_w/M_n{}^c$
homopolymer	84.5		1.08
N8515	84.5	15.1	1.15
N8530	84.5	31.1	1.18
N8545	84.5	44.5	1.21
N8560	84.5	60.1	1.23

[a] Obtained by mass spectrum for the homopolymer and assumed to have the same value as for the block copolymers. [b] ^{1}H NMR. [c] GPC.

The copolymers were hydrolyzed by sodium hydroxide in dioxane and led to HOVE−NBVE block copolymers. These were purified by dialysis with deionized water, and their aqueous solutions were passed through a filter with a pore size of 0.22 μm.

Molecular Characterization. The values of M_w/M_n were determined by GPC (solvent: chloroform) with a polystyrene standard calibration for AcOVE−NBVE block copolymers, where M_w and M_n are the weight- and number-averaged molecular weights, respectively. We obtained the number-averaged degree of polymerization of AcOVE (m) to be 84.5 from the mass spectrum of the homopolymer and assumed that four block copolymers synthesized simultaneously have the same value of m. The degree of polymerization of NBVE (n) was evaluated by comparing the area of methyl peaks of both acetoxyl and butyl groups obtained by ^{1}H NMR. These values are listed in Table 1. Although they were evaluated for poly(AcOVE-*b*-NBVE) precursor polymers, they can be applied for poly(HOVE-*b*-NBVE) polymers as well, since we confirmed by ^{1}H NMR that no subreaction had taken place during hydrolysis, such as polymer degradation process. The ^{1}H NMR spectrum of poly(HOVE-*b*-NBVE) with $m = 85$ and $n = 15$ (N8515) in D_2O is shown in Figure 1. It shows no acetoxy peak, indicating that the protective groups were completely hydrolyzed and removed by purification. In addition, a relatively broad peak derived from the methyl protons of butyl groups is observed at 0.8 ppm, reflecting the fact that the hydrophobic

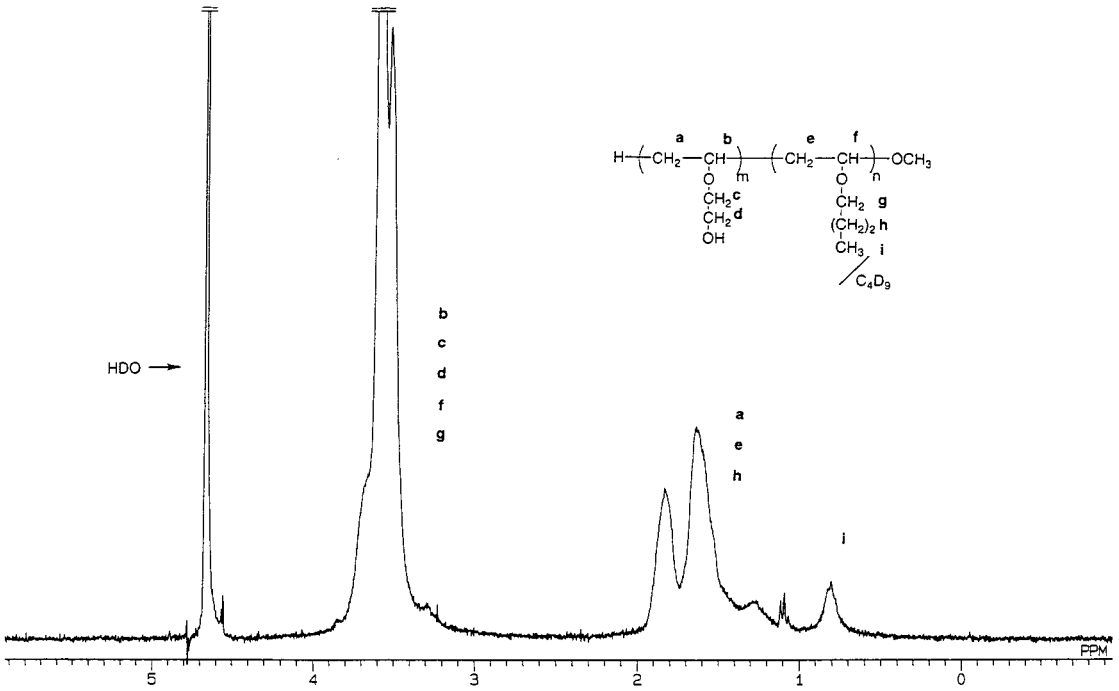

Figure 1. ^{1}H NMR spectrum of poly(HOVE-*b*-NBVE) in D_2O.

part tends to avoid contact with water molecules, which is evidence of micelle formation in water.

Small-Angle Neutron Scattering. The SANS measurements were performed by the KWS1 spectrometer at the research reactor FRJ2 at the Forschungszentrum Jülich GmbH. The wavelength (λ) of neutron source was chosen to be 7 Å ($\Delta\lambda/\lambda = 20\%$). Solutions were measured in quartz cells with a path length of 1 and 2 mm. The SANS experiments were carried out at a sample to detector distance of 2, 4, 8, and 20 m, covering a range of the scattering vector of $0.002 \leq q \leq 0.1$ Å^{-1}. Scattering data measured by a 2D detector were circular averaged to be 1D form scattering data and then corrected for electronic background, and the scattering of the empty cell was subtracted. The data were transformed to absolute cross sections using a Lupolen standard. For all scattering data of samples, the scattering of solvent and the calculated incoherent scattering of the protonated portion of the polymer were subtracted.

For measurements by the contrast variation method, we used D_2O/H_2O solvent mixtures. Four different volume fractions of D_2O (ϕ_{D_2O}) were chosen for each polymer solution to obtain various contrasts:

$$\phi_{D_2O} = 0 \text{ (H_2O contrast)}$$

$$\phi_{D_2O} = 0.199 \text{ (core contrast, where } \rho_0 = \rho_{HOVE})$$

$$\phi_{D_2O} = 0.350 \text{ (intermediate contrast)}$$

$$\phi_{D_2O} = 0.500 \text{ (shell contrast, where } \rho_0 = \rho_{NBVE})$$

For the calculation of the core and the shell contrasts, the molar volumes of NBVE (105.54 cm^3/mol) and HOVE (75.56 cm^3/mol) corresponding to the measured densities of homopolymer NBVE (0.949 g/cm^3) and HOVE (1.166 g/cm^3) were used. The volume fraction of polymer was chosen to be 1% for all measurements, except for the investigation of the concentration dependence.

3. Theoretical Background

If the contribution of interparticle interaction is negligible, the neutron scattering cross section can be given by the equation

$$d\Sigma(q)/d\Omega = n_p P(q) \quad (1)$$

where n_p is the number density of particles and $P(q)$ is the particle form factor. The scattering vector q is given by $q = 4\pi \sin\theta/\lambda$, where 2θ is the scattering angle and λ is the neutron wavelength. $P(q)$ depends on the size, shape, and density distribution inside the scattering particles.

Here we deal with two models for describing the SANS data, spherical and cylindrical ones. In both cases, we assumed that the micelles consist of a core−shell structure. The form factor of a spherical core−shell model with the radii of the core R_C and of the overall micelle R_S can be written as follows:[17]

$$P(q)_{sphere} = \{(\rho_C - \rho_S)V_C F_C(q)_{sphere} + (\rho_S - \rho_0)V_S F_S(q)_{sphere}\}^2 \quad (2)$$

$$F_C(q)_{sphere} = 3(\sin(qR_C) - qR_C\cos(qR_C))/(qR_C)^3 \quad (3)$$

$$F_S(q)_{sphere} = 3(\sin(qR_S) - qR_S\cos(qR_S))/(qR_S)^3 \quad (4)$$

where ρ_C, ρ_S, and ρ_0 are the SLDs of the core, the shell, and the solvent. V_C and V_S are given as $4\pi R_C{}^3/3$ and $4\pi R_S{}^3/3$, respectively. The aggregation number (N_{agg}) is calculated from V_C, n, and the volume of NBVE repeat unit (v_{NBVE}):

$$N_{agg} = \phi_p V_C/(n v_{NBVE}) \quad (5)$$

where ϕ_p is the volume fraction of polymer in the core and is equal to 1 for the close-packed core. The volume occupied by hydrophilic parts of polymers in the shell of a micelle is given by ($N_{agg} m v_{HOVE}$), where v_{HOVE} is the volume of the HOVE repeat unit. Thus, the volume fraction of polymer in the shell (ϕ_S) is calculated as

$$\phi_S = N_{agg} m v_{HOVE}/(V_S - V_C) \quad (6)$$

then ρ_0, ρ_C, and ρ_S are given by the SLDs of D_2O (ρ_{D_2O}), H_2O (ρ_{H_2O}), NBVE (ρ_{NBVE}), and HOVE (ρ_{HOVE}):

$$\rho_0 = \phi_{D_2O}\rho_{D_2O} + (1 - \phi_{D_2O})\rho_{H_2O} \quad (7)$$

$$\rho_C = \phi_p\rho_{NBVE} + (1 - \phi_p)\rho_0 \quad (8)$$

$$\rho_S = \phi_S\rho_{HOVE} + (1 - \phi_S)\rho_0 \quad (9)$$

where ϕ_{D_2O} is the volume fraction of D_2O in solvent. Here the SLDs of repeat units and pure solvent can be calculated as

$$\rho_i = \sum b_Z/v_i \quad (10)$$

where subscript i refers to D_2O, H_2O, NBVE, or HOVE. b_Z is the scattering length of atom z in the repeat unit or solvent molecule, and v_i is the corresponding volume. Thus, $\rho_{D_2O} = 6.406 \times 10^{10}$ and $\rho_{H_2O} = -5.617 \times 10^9$ cm^{-2} can be obtained. One can obtain the values of ρ_{NBVE} and ρ_{HOVE} if the densities of NBVE and HOVE are determined. For the calculation of ρ_{HOVE}, the isotopic exchange of the hydrogen in the OH group of HOVE should be taken into account, by assuming that this hydrogen is occupied by a deuterium or hydrogen in proportion to ϕ_{D_2O}.

In the case of a core−shell cylinder with the radii of the core R_C and the overall micelle R_S and the length L, its form factor is given by[17]

$$P(q)_{cylinder} = (1/2)\int_0^{\pi}\{(\rho_C - \rho_S)V_C F_C(q)_{cylinder} + (\rho_S - \rho_0)V_S F_S(q)_{cylinder}\}^2 \sin\beta\, d\beta \quad (11)$$

$$F_C(q)_{cylinder} = \{(\sin(q(L/2)\cos\beta)/(q(L/2)\cos\beta)\} \times \{2J_1(qR_C\sin\beta)/(qR_C\sin\beta)\} \quad (12)$$

$$F_S(q)_{cylinder} = \{(\sin(q(L/2)\cos\beta)/(q(L/2)\cos\beta)\} \times \{2J_1(qR_S\sin\beta)/(qR_S\sin\beta)\} \quad (13)$$

where β is the angle between the axis of symmetry of cylinder and the scattering vector q and J_1 denotes the Bessel function of the first kind and of order 1. V_C and V_S are the volumes of cylinders with radii R_C and R_S, respectively, and length L.

On the condition that $q \gg 2\pi/L$ and $L \gg R_S$, the form factor of cylinder can be modified to a simpler form:

$$P(q)_{cylinder} = (\pi/qL)\{(\rho_C - \rho_S)V_C 2J_1(qR_C)/(qR_C) + (\rho_S - \rho_0)V_S 2J_1(qR_S)/(qR_S)\}^2 \quad (14)$$

The same equation as eqs 5−9 can apply to the cylinder for calculation of N_{agg}, ϕ_S, and the SLDs. The neutron wavelength distribution ($\Delta\lambda/\lambda = 20\%$) and collimation

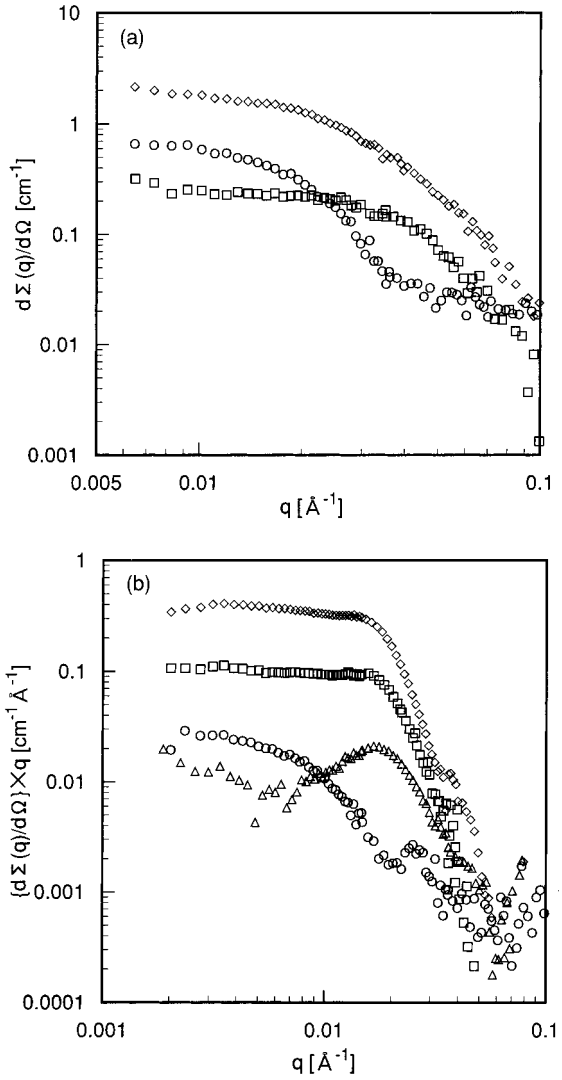

Figure 2. (a) Scattering cross sections of N8515 and (b) Holtzer plots of N8560 under several contrast conditions: H_2O (◇), core (□), intermediate (△), and shell contrast (○).

of the SANS machine were taken into account in the data evaluation.[18]

4. Results and Discussion

Figure 2 shows the SANS profiles of aqueous solutions of N8515 and N8560 at several contrasts. As shown in Figure 2a, the profiles for N8515 which has the shortest hydrophobic length exhibited a plateau at a smaller angle that is typical for spherical particles. For N8560 having the longest NBVE chain, the profiles were quite different from those of N8515 as shown in Figure 2b. Notice that the y axis in Figure 2b is the absolute scattering intensity multiplied by q. The q^{-1} dependence of the scattering intensities can be clearly found at a smaller angle, which is characteristic of rodlike particles. This q^{-1} dependence was observed for N8545 as well. A tendency that the SANS profile depends on the polymer composition has been also observed previously.[19]

It is clear experimentally from the scattering profiles and also theoretically from eq 2 that the forward scattering intensity ($d\Sigma(q=0)/d\Omega$) depends on the SLD of solvent (ρ_0) and that the square root of the forward scattering intensity is proportional to ϕ_{D_2O}.[20] For N8515 and N8530, the determination of the forward scattering

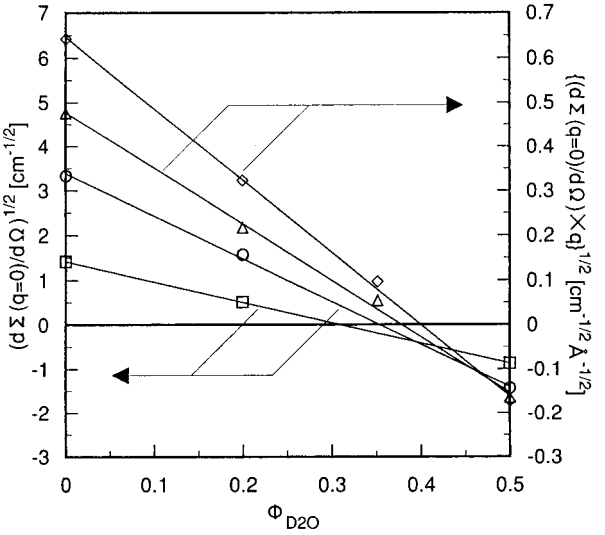

Figure 3. Square root of forward scattering intensity plotted against the volume fraction of D_2O: N8515 (□), N8530 (○), N8545 (△), and N8560 (◇). For the latter two cases, $\{(d\Sigma(q=0)/d\Omega) \times q\}^{1/2}$ is plotted instead of forward scattering intensity. The solid lines are due to least-squares fits, and the crossing point with $y = 0$ is zero average contrast (ϕ_{ZAC}).

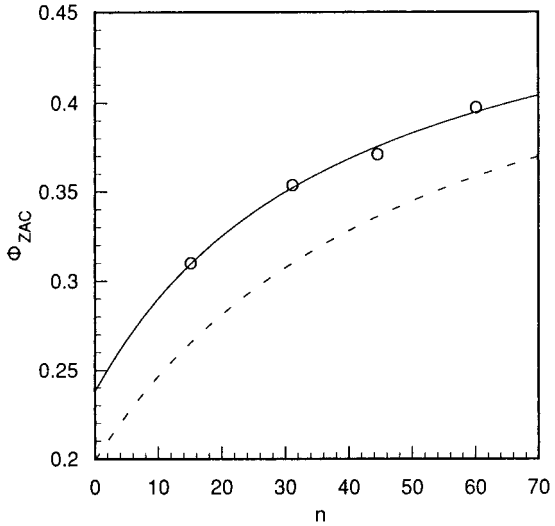

Figure 4. Dependence of ϕ_{ZAC} obtained from Figure 3 on hydrophobic chain length. The broken line is due to eq 16 with the values of $v_{NBVE} = 105.54$ and $v_{HOVE} = 75.56$ cm^3/mol. The solid line shows the fitted results obtained by changing v_{NBVE} and v_{HOVE} as fitting parameters.

intensity for each contrast was possible by a linear extrapolation of a Guinier plot[17] ($\ln(d\Sigma(q)/d\Omega) \sim q^2$ plot). The plots of the square root of these forward scattering intensities against ϕ_{D_2O} gave a good linear relationship as can be seen in Figure 3. For N8545 and N8560, however, it is impossible to determine the forward scattering intensity because of the q^{-1} dependence at a small angle as described above. However, the value of $d\Sigma(q=0)/d\Omega \times q$ can be obtained instead of $d\Sigma(q=0)/d\Omega$ by linear extrapolation of $\ln(d\Sigma(q)/d\Omega \times q) \sim q^2$ plot,[10] and similarly, a good linear relationship between $(d\Sigma(q=0)/d\Omega \times q)^{1/2}$ and ϕ_{D_2O} was found as shown in Figure 3. The volume fraction of D_2O at $d\Sigma(q=0)/d\Omega = 0$ or $(d\Sigma(q=0)/d\Omega \times q = 0$ (ϕ_{ZAC}) was determined for each polymer by least-squares fits and is plotted against n (NBVE length) in Figure 4. At the zero average contrast condition $\phi_{D_2O} = \phi_{ZAC}$, the SLD of solvent mixture coincides with the averaged SLD of the copolymer:

$$\phi_{ZAC}\rho_{D_2O} + (1 - \phi_{ZAC})\rho_{H_2O} = (mb_{HOVE} + nb_{NBVE})/(mv_{HOVE} + nv_{NBVE}) \quad (15)$$

where b_{HOVE} and b_{NBVE} are the scattering lengths of HOVE and NBVE, respectively. Modifying eq 15, ϕ_{ZAC} can be represented as a function of n:

$$\phi_{ZAC}(n) = \{(mb_{HOVE} + nb_{NBVE})/(mv_{HOVE} + nv_{NBVE}) - \rho_{H_2O}\}/(\rho_{D_2O} - \rho_{H_2O}) \quad (16)$$

Note that the value of b_{HOVE} depends on the solvent composition due to the isotopic exchange of the hydrogen as described above. The broken line in Figure 4 is derived from eq 16 with the values of 105.54 and 75.56 cm^3/mol as the molar volumes of NBVE and HOVE, respectively. A large discrepancy was observed between the broken line and experimental data. Then, we tried to fit the experimental data by eq 16 changing v_{NBVE} and v_{HOVE} as fitting parameters. As a result, we obtained the molar volumes of NBVE of 105.62 and HOVE of 59.13 cm^3/mol and found good agreement with experimental data as shown by the solid line in Figure 4. For NBVE, nearly the same molar volume was obtained as expected. On the other hand, the molar volume of 59.13 cm^3/mol for HOVE, which corresponds to the density 1.490 g/cm^3, is considerably small. This means that the partial molar volume of HOVE in water is smaller than the molar volume of its own molar volume in bulk state. It is well-known that when a hydrophobic substance is put in water, water forms a highly structurized "iceberg" surrounding the hydrophobic molecule.[21] The decrease of the partial molar volume can be explained as apparent deletion of the volume of methylene groups which are located in the main chain or side chain of HOVE, by movement of the methylene into a vacancy inside of the iceberg. This phenomenon, for example, is also observed as the decrease of total volume when water and ethanol are mixed. This hydration effect is important and must be taken into account to describe the data.[12] The densitometric measurements of the partial specific volume of the copolymers and HOVE homopolymer in water will also give us an important information about the hydrophobic interaction in the shell, which is under investigation.

We used the calculated molar volumes (105.62 and 59.13 cm^3/mol for NBVE and HOVE, respectively) and fitted the data for all contrast conditions, simultaneously. For N8515, using the spherical core−shell model, we found good agreement between experimental and theoretical data as can be seen in Figure 5. However, we had to introduce the value of $\phi_p = 0.72$ to describe the data, suggesting the existence of water in the micellar core; otherwise, we could not fit the data on an absolute scale. It can be concluded that NBVE which has an ether bonding may permit the penetration of water into the core to some extent. The obtained values of the micellar structure parameters are listed in Table 2.

Since the q^{-1} dependence of the scattering intensities was clearly observed for N8560, the core−shell cylindrical model was first applied. It is impossible to determine the length or total volume of the rod, because it is possible only when the deviation from the q^{-1} slope and so-called Guinier region are observed. Then eq 14 is

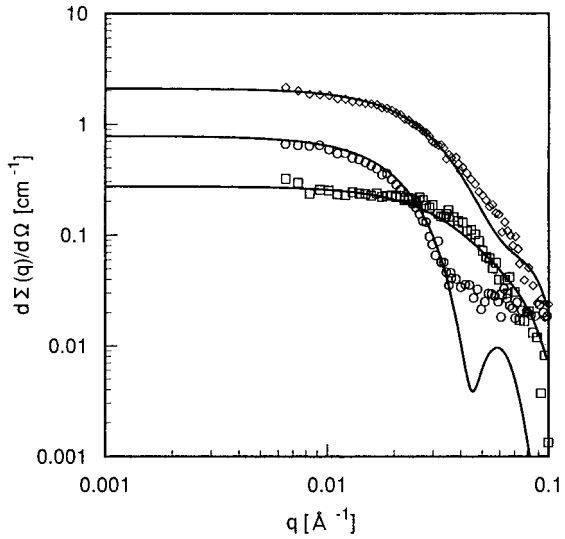

Figure 5. Scattering cross sections of N8515. The same symbols are used as in Figure 2. The solid lines represent the theoretical curves of the core−shell spherical model.

Table 2. Parameters of Sphere−Rod Coexistence Model

				sphere		rod	
	R_C (Å)	R_S (Å)	ϕ_{rod}	N_{agg}	ϕ_S	N_{agg}/L (Å^{-1})[a]	ϕ_S
N8515	36	98	0	53	0.12		
N8530	68	145	0.05	174	0.13	1.92	0.30
N8545	88	170	0.15	263	0.12	2.24	0.27
N8560	110	200	0.30	381	0.11	2.60	0.23

[a] The aggregation number of rodlike micelles per unit length.

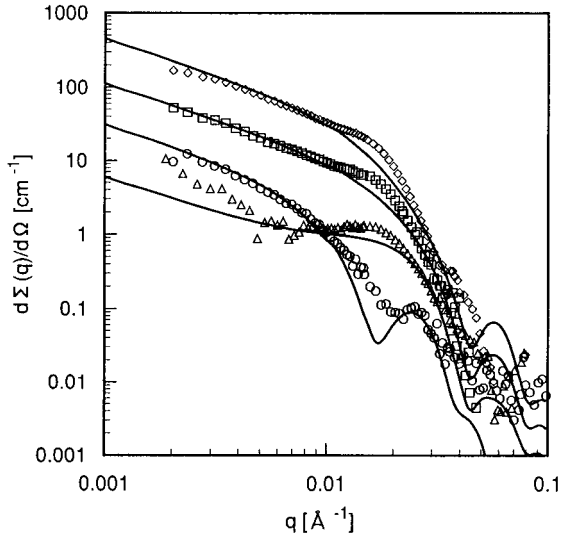

Figure 6. Scattering cross sections of N8560. The same symbols are used as in Figure 2. The solid lines represent the theoretical curves of the core−shell cylindrical model.

sufficient and was used for fitting the data. However, the agreement between experimental and theoretical profiles was not satisfactory as shown in Figure 6. The theoretical curves of the cylinder properly showed the q^{-1} dependence and was consistent with the experimental data at a smaller angle. However, in the region $q \approx 0.02$ Å^{-1} where the scattering intensity deviates from the straight line with a slope of −1, the two curves do not fit each other.

Then, we introduced a new assumption that not only the rodlike micelles but also the spherical micelles

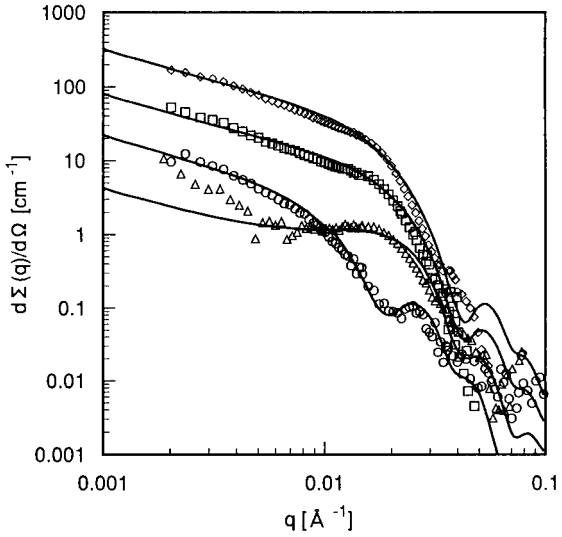

Figure 7. Scattering cross sections of N8560 with the fitted curve using coexisting model.

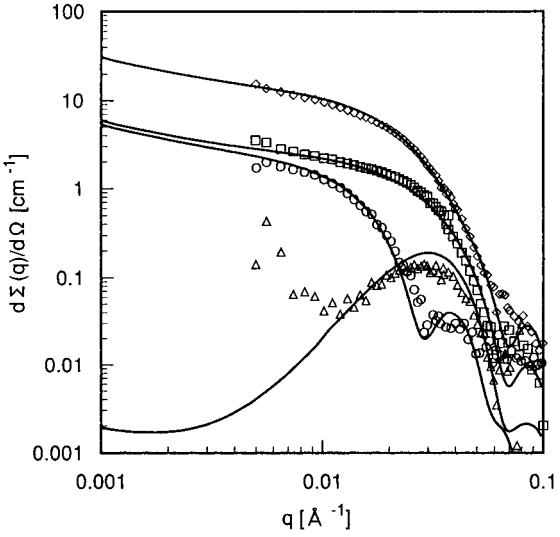

Figure 8. Scattering cross sections of N8530 with the fitted curve using coexisting model.

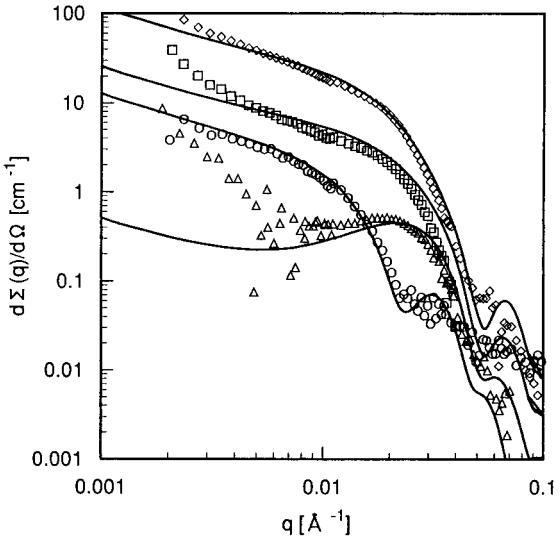

Figure 9. Scattering cross sections of N8545 with the fitted curve using coexisting model.

coexist in the solution of N8560. This sphere−rod coexistence model can be satisfied by this form factor with eqs 2 and 14:

$$P(q)_{\mathrm{mix}} = \phi_{\mathrm{Nrod}} P(q)_{\mathrm{cylinder}} + (1 - \phi_{\mathrm{Nrod}}) P(q)_{\mathrm{sphere}} \quad (17)$$

where ϕ_{Nrod} is the number fraction of the rodlike micelles in the total number of micelles in the solution. It is more convenient to use the volume fraction of the rodlike micelles ϕ_{rod} which relates to ϕ_{Nrod}:

$$\phi_{\mathrm{Nrod}} = \phi_{\mathrm{rod}}/\{\phi_{\mathrm{rod}} + (1 - \phi_{\mathrm{rod}})(N_{\mathrm{agg,\,rod}}/N_{\mathrm{agg,\,sphere}})\} \quad (18)$$

Here $N_{\mathrm{agg,\,rod}}$ and $N_{\mathrm{agg,\,sphere}}$ are the aggregation numbers of the rodlike micelles and the spherical micelles, respectively. If all the polymers in the solution can be assumed to participate in the micelles, i.e., the critical micellar concentration is considerably low, ϕ_{rod} is identical to the number fraction of polymers contributing to the formation of the rodlike micelles. In this model, radial dimensions are identical for the spherical and the rodlike micelles, that is, $R_{\mathrm{C,\,rod}} = R_{\mathrm{C,\,sphere}}$ and $R_{\mathrm{S,\,rod}} = R_{\mathrm{S,\,sphere}}$.

The fitting results for N8560 with the coexistence model are shown in Figure 7. A marked improvement of fitting quality was obtained compared with the core−shell cylindrical model. The obtained model parameters are listed in Table 2.

Using the same model, the scattering curves of N8530 and N8545 micelles were fitted as shown in Figures 8 and 9. In all cases, the value of $\phi_{\mathrm{p}} = 0.72$ was fixed, and good agreement was achieved on an absolute scale. The obtained model parameters are listed in Table 2. As a result, we found an increase of micellar size (R_{C}, R_{S}, or N_{agg}) with increasing hydrophobic chain length of block copolymer. In addition, rodlike aggregates started to form, and their volume fraction increased by the elongation of the hydrophobic chain. The rodlike micelles could have a broad distribution of lengths, but the averaged length should be quite large (at least 5000 Å) from the fact that the Guinier region could not be observed in the experimental q range. We were not able to determine the length distribution of rod since the consideration of the length distribution of the rod made no change on SANS profiles in the experimental q range.

It should be also noticed that at least 70% of molecules contribute to the formation of spherical micelle. It means that a large number of spherical micelles coexist with a small number of rodlike micelles which have extremely large dimensions and a broad distribution of lengths. Other models such as pure cylinder or ellipsoid with the length distribution will reproduce neither the micellization tendency nor the experimental SANS profiles. Other approaches such as electron microscopy will provide this information and prove the coexistence model.

Although there have been many examples of sphere to rod transition for the triblock copolymer system such as poly(ethylene oxide)−poly(propylene oxide)−poly(ethylene oxide) (PEO−PPO−PEO) in water at elevated temperatures,[13,22] the rodlike micelle formation of diblock copolymers at a low concentration and low temperature in water which we presented here should be noted. Zhang and Eisenberg have used electron microscopy and found the "crew-cut" micelles of multiple morphologies of polystyrene-*block*-poly(acrylic acid) including rodlike structure.[23] Zhao et al. have also reported the rodlike micelle of polystyrene-*block*-poly(*p*-hydroxystyrene)

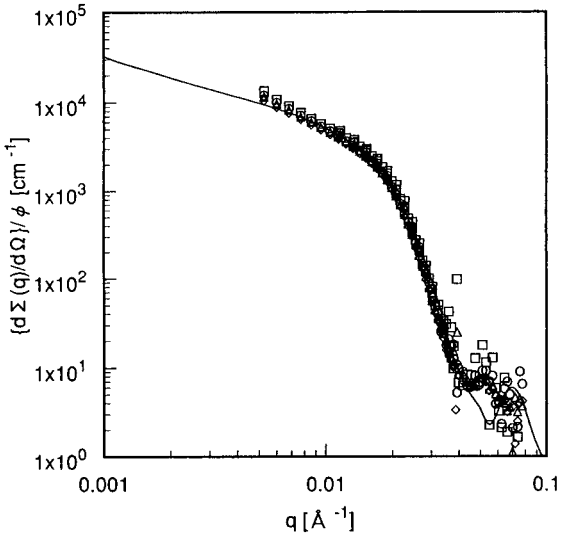

Figure 10. Scattering cross sections of N8545 in D_2O normalized by polymer concentration: 0.05% (□), 0.1% (○), 0.2% (△), and 0.5% (◇). The solid line is the theoretical curve with the same parameters as used in Figure 9.

formed in toluene by a combination of both static and dynamic light scattering studies.[24] These are rare examples of the rodlike micelles of diblock copolymer, and the methods that they used for the investigation could be applicable to our system and might be complementary to the SANS data.

The transition behavior can be qualitatively understood from the concept of "critical packing parameter" introduced by Israelachvili[25] for low molecular weight surfactants. If the hydrophobic chain length keeps on increasing in the spherical micelle, the area occupied by the polymer at the core−shell interface increases. However, there is an upper limit to the area that can be covered by a hydrophilic chain with a certain length. Therefore, transition to a rod shape will occur when the interfacial area per molecule of the spherical micelle exceeds this limit by the increase of the hydrophobic chain length.

The concentration dependence of the SANS profile was investigated for N8545. To obtain the highest intensity (contrast), D_2O was used as a solvent, and the polymer volume fraction was varied from 0.05 to 0.5%. The data were normalized by the polymer volume fraction. We expected that the decrease in the concentration would shorten the length of the rodlike micelle, thereby making the total micellar size detectable, or reduce the volume fraction of the rod, but the SANS data were independent of the concentration as can be seen in Figure 10. The normalized data were reproduced by the calculated curve with the same parameters as used in Figure 9. This suggests that the rodlike micelle with an extremely long dimension already exists at a considerably low concentration and that the volume fraction of rod does not change at least up to 1%.

No cloud point for the 1% solution of these copolymers was observed when we increased the temperature up to 90 °C. In the case of the PEO−PPO−PEO triblock copolymer, a strong temperature dependence of the phase behavior such as sphere to rod transition or phase separation has been observed.[13,22,26] Since the copolymers we used have OH groups at the side chains of the hydrophilic chain, which can effectively interact with the solvent, the hydrogen bond may not be broken even by frequent thermal motion of the polymer, and phase separation may not occur even at a high temperature. However, further studies are required on the dependence of rodlike aggregates on temperature or concentration. Moreover, a theoretical approach[26,27] is necessary to interpret the phenomena experimentally observed. These studies are now in progress.

5. Conclusions

Amphiphilic diblock copolymers poly(HOVE-*b*-NBVE) with a partially deuterated hydrophobic segment were synthesized by living cationic polymerization and subsequent hydrolysis. These copolymers formed micelles in an aqueous solution. The internal structure of the micelles was investigated by the contrast variation method of SANS measurements. The molar volume of HOVE obtained by calculation of zero average contrast was quite small, which results from the hydration effect in the micellar shell. The SANS curves were described by the core−shell model. The micellar shape was strongly dependent on the hydrophobic chain length of the polymer. The polymer with the shortest hydrophobic chain was suggested to form spherical micelles. With increasing hydrophobic chain length, rodlike micelles started to form, and their volume fraction was increased.

Acknowledgment. We gratefully acknowledge the support of a Grant for Joint Research Project under the Japanese−German Cooperative Science Promotion Program from both Japan Society for the Promotion of Science and Deutsche Forschungsgemeinschaft.

References and Notes

(1) Halperin, A.; Tirrell, M.; Lodge, T. P. *Adv. Polym. Sci.* **1992**, *100*, 31.
(2) Chu, B. *Langmuir* **1995**, *11*, 414.
(3) Tuzar, Z.; Kratochvil, P. *Advances in Colloid and Interface Science*; Elsevier: Amsterdam, 1976.
(4) Zana, R. *Colloid Surf. A: Physicochem. Eng. Aspects* **1997**, *123−124*, 27.
(5) Grubbs, R. H.; Tumas, W. *Science* **1989**, *243*, 907.
(6) Miyamoto, M.; Sawamoto, M.; Higashimura, T. *Macromolecules* **1984**, *17*, 265.
(7) Sawamoto, M. *Prog. Polym. Sci.* **1991**, *16*, 111.
(8) Mortensen, K.; Brown, W. *Macromolecules* **1993**, *26*, 4128.
(9) Magid, L. J. *Nonionic Surfactants*; Marcel Dekker: New York, 1987; Vol. 23.
(10) Herbst, L.; Kalus, J.; Schmelzer, U. *J. Phys. Chem.* **1993**, *97*, 7774.
(11) Yamaoka, H.; Matsuoka, H.; Sumaru, K.; Hanada, S.; Imai, M.; Wignall, G. D. *Physica B* **1995**, *213&214*, 700.
(12) Poppe, A.; Willner, L.; Allgaier, J.; Stellbrink, J.; Richter, D. *Macromolecules* **1997**, *30*, 7462.
(13) Mortensen, K. *J. Phys.: Condens. Matter* **1996**, *8*, A103.
(14) Cantor, C. R.; Schimmel, P. R. *Biophysical Chemistry, Part II: Techniques for the Study of Biological Structure and Function*; W. H. Freeman and Co.: San Francisco, 1980.
(15) Higgins, J. S.; Benoit, H. C. *Polymers and Neutron Scattering*; Oxford: New York, 1996.
(16) McKeon, J. E.; Fitton, P. *Tetrahedron* **1972**, *28*, 233.
(17) Guinier, A.; Fournet, G. *Small-Angle Scattering of X-rays*; John Wiley: New York, 1955.
(18) Pedersen, J. S.; Posselt, D.; Mortensen, K. *J. Appl. Crystallogr.* **1990**, *23*, 321.
(19) Nakano, M.; Matsuoka, H.; Yamaoka, H.; Poppe, A.; Richter, D. *Physica B* **1998**, *241−243*, 1038.
(20) Ibel, K.; Stuhrmann, H. B. *J. Mol. Biol.* **1975**, *93*, 255.
(21) Frank, H. S.; Evans, M. W. *J. Chem. Phys.* **1945**, *13*, 507.
(22) Schillén, K.; Brown, W.; Johnsen, R. M. *Macromolecules* **1994**, *27*, 4825.
(23) Zhang, L.; Eisenberg, A. *Science* **1995**, *268*, 1728.
(24) Zhao, J. Q.; Pearce, E. M.; Kwei, T. K.; Jeon, H. S.; Kesani, P. K.; Balsara, N. P. *Macromolecules* **1995**, *28*, 1972.
(25) Israelachvili, J. N. *Intermolecular and Surface Forces*, 2nd ed.; Academic Press: London, 1985.
(26) Linse, P. *J. Phys. Chem.* **1993**, *97*, 13896.
(27) Munch, M. R.; Gast, A. P. *Macromolecules* **1988**, *21*, 1360.

MA981351P